Dalton Transactions

Accepted Manuscript

ROYAL SOCIETY OF CHEMISTRY

www.rsc.org/dalton

TOC

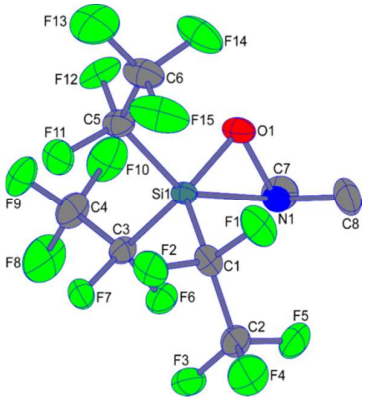

Pentafluoroethyl-substituted *α*-silanes: model compounds for new insights

B. Waerder, S. Steinhauer, J. Bader, B. Neumann, H.-G. Stammler, Yu. V. Vishnevskiy, B. Hoge and N. W. Mitzel*

A joint experimental/computational approach addresses the question on occurrence and nature of bonds between Si and N atoms in $(C_2F_5)_3Si\text{-}X\text{-}NMe_2$ (X = CH_2, O).

Journal Name

RSCPublishing

ARTICLE

Pentafluoroethyl-substituted α-silanes: model compounds for new insights

Cite this: DOI: 10.1039/x0xx00000x

Benedikt Waerder,[a] Simon Steinhauer,[a] Julia Bader,[a] Beate Neumann,[a] Hans-Georg Stammler,[a] Yury V. Vishnevskiy,[a] Bert Hoge[a] and Norbert W. Mitzel*[a]

Received 00th January 2014,
Accepted 00th January 2014

DOI: 10.1039/x0xx00000x

www.rsc.org/

To further investigate the α-effect in silanes bearing a geminal donor atom, the model compounds $(C_2F_5)_3SiCH_2NMe_2$, $(C_2F_5)_3SiCH_2OMe$ and $(C_2F_5)_3SiONMe_2$ were prepared by introduction of pentafluoroethyl groups via nucleophilic substitution of the corresponding chloro-derivatives with pentafluoroethyl lithium. The substances were characterised by NMR spectroscopy and X-ray diffraction via *in-situ* crystallization techniques. The solid state structures of these highly electronegatively substituted α-silanes contain monomeric molecules. The Si–C–N angle in $(C_2F_5)_3SiCH_2NMe_2$ shows a value of 115.3(2)° and the Si–C–O angle in $(C_2F_5)_3SiCH_2OMe$ a value of 105.4(1)°. Both values are smaller than the Si–C–C angle of the reference compound $(C_2F_5)_3SiCH_2CH_3$ with a value of 118.6(2)° indicating attractive interaction between the silicon atom and the respective donor atoms. The Si–O–N angle in $(C_2F_5)_3SiONMe_2$ is extremely narrow at 82.0(1)°. This behaviour was further investigated by gas electron diffraction and by quantum-chemical calculations. The NBO method finds no significant orbital interactions between Si and N/O atoms in the Si–C–N, Si–C–O and Si–O–N units. The IQA model describes the compounds as strongly stabilised by electrostatic interactions between formally non-bonded silicon and donor atoms.

Introduction

For almost 50 years, it has been discussed that silicon compounds carrying a donor atom in β position (substituents at α-position) have different chemical, structural and physical properties compared to their carbon analogues.[1,2,3,4] The early picture of the so-called α-effect is a classical dative bond between a silicon atom and a geminal donor centre. It was introduced by Kostyanovski[5] in order to rationalize the reactivity and properties of such geminal systems.[6] Industrial use of this effect is made in the accelerated hydrolysis in the class of so-called α-silanes as surface mediators, cross-linking agents and other useful industrial products.[7] Driven by these important applications, hydrolysis of α-silanes has intensely investigated by kinetic and theoretical methods revealing that the whole process is much more complicated than the original picture of the α-effect.[7,8] Tacke and co-workers come to the conclusion that *the term "silicon α-effect" should not be used furthermore to explain the hydrolysis reactivity at the silicon atom of alkoxyorganylsilanes with functional groups in α- or γ-position*.[8] However, fundamental interaction types have to be clearly distinguished from the complex interplay of reactants involving solvation, pre-aggregation and many more polarity or dipole-driven effects in solution.

For some model compounds for the classical α-effect, with a bridging group between silicon an donor atom being an oxygen or nitrogen atom, extreme structure deviations were observed: e.g. acute bond angles of 77.1(1)° at the oxygen atom were for $F_3SiONMe_2$[9] and 74.1(1)° for $(CF_3)F_2SiONMe_2$[10], both in the solid state, whereas these parameters are larger in the gas phase for free molecules (94.3(9)° and 87.1(9)°).

Charge density analyses for $F_3SiONMe_2$[9] and $(CF_3)F_2SiONMe_2$[10] have shown, that despite the clearly attractive interactions between Si and N atoms, there is no associated bond path or bond critical point the sense of the Quantum Theory of Atom in Molecules[11] and the Laplacian of Electron density shows no clear charge depletion on the silicon atom oriented to the nitrogen atom, while the nitrogen atom has a local charge accumulation, that is not exactly oriented to the silicon atom. The situation is paralleled by that in BCN three-membered rings with dative B···N bond,[12] despite three ring angles being close to 60°: no B···N bond-path, no ring topology in the charge density. This has been attributed to the special situation in three-membered rings with one weaker bond: the importance of the close proximity of a third atom for the charge density topology in the region of the weak bond.

In contrast to the situation in SiON and SiNN[13] compounds, no clear indications for an attractive interaction between silicon

and donor atoms were found with methylene bridges. For F_3SiCH_2OMe, for instance, attractive interactions could neither be detected in the solid state nor in the gas phase.[14] Quantum-chemical investigations also yielded no indication for interactions between the silicon and the oxygen atoms.

For $F_3SiCH_2NMe_2$, a simple model for the commercially used aminomethylsilanes (type SiCN), more extensive theoretical studies were conducted in addition to the structural investigations. A markedly flattened energy potential for the Si–C–N angle, in particular at values lower than the equilibrium structure have been reported.[15] Further investigations like AIM (quantum theory of atoms in molecules[11]) and NBO (natural bond orbital) analyses[16] have given no indication of interactions between the silicon and nitrogen atoms. Experimentally it has been found that $F_3SiCH_2NMe_2$ forms a dimer in the solid state, bridged by Si–N contacts. In the gas phase, however, neither intermolecular nor intramolecular Si–N interactions have been found.

Model compounds with one fluorine atom being replaced by the sterically more bulky C_6F_5 group yielded the first solid state structure of a monomeric model compound with a Si–C–N motif:[17] the Si–C–N angle in $(C_6F_5)F_2SiCH_2NMe_2$ is 107.0(3)° and direct orbital interactions between the silicon and nitrogen atoms have been excluded on the basis of NBO calculations. It has been concluded that the observed structures and the flat bending potentials of such compounds, derived from quantum-chemical investigations, were due to electrostatic interactions and dipolar behaviour.

To shed some more light onto this complex topic, we prepared a series of new model compounds with pentafluoroethyl groups instead of fluorine atoms, which we report here. Pentafluoroethyl groups have a high electronegativity and are not capable of back-bonding. Further advantages of the pentafluoroethyl groups are their higher thermal stability compared to trifluoromethyl groups. Their high steric demand[18] should suppress dimerization of the products.[19]

Pentafluoroethyl groups can be easily introduced using the reagent pentafluoroethyllithium,[20] which has just recently been structurally elucidated.[21] Hoge and co-workers have recently reported highly reactive halosilanes and even tris(pentafluoroethyl)dichlorosilicates that can be stabilised with these substituents, yielding very acidic silicon sites, which would be a favourable characteristic in our present investigations of internal donor-acceptor bonding.[22,23]

Results and discussion

Synthesis

The series of model compounds reported here are all of the type $(C_2F_5)_3Si–A–X$, with A being a spacer and X being a donor atom. For the first group of compounds, $(C_2F_5)_3SiCH_2OMe$ and $(C_2F_5)_3SiCH_2NMe_2$, with A = CH_2, a reference compound without donor, $(C_2F_5)_3SiCH_2CH_3$ (X = CH_3), was investigated as a benchmark for our new compounds. This was necessary since each class of previously investigated compounds used very different substituents at the silicon atom, so that a direct comparison of structural parameters to those of our new compounds with sterically demanding electron-withdrawing groups could involve problems. For comparison of the bonding situation in previously investigated three-membered rings containing a silicon atom, we synthesised a compound with A = O and X = NMe_2: $(C_2F_5)_3SiCH_2OMe$.

All compounds were prepared starting from the respective trichloro derivatives $Cl_3Si–A–X$, which were either commercially available or prepared according to literature. These chlorosilanes were reacted with pentafluoroethyl lithium, which was generated *in situ* (Scheme 1).

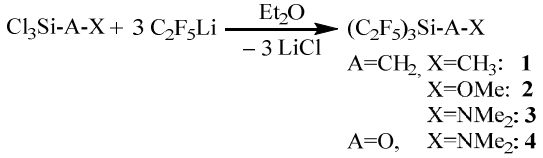

Scheme 1: Preparation of compounds **1** – **4**

Interestingly, compound **3** could also be obtained via an alternative synthetic pathway, the reaction of $(C_2F_5)_3SiF$ with NMe_3. In analogy to the formation of similar phosphane derivatives, we propose the reaction sequence in Scheme 2 for this reaction. It involves hydride abstraction as a first step, which is not unlikely regarding the extreme Lewis acidity of $(C_2F_5)_3SiF$.[24] The formation of $[Me_3NH][(C_2F_5)_3F_2Si]$ was proven by comparison of the NMR spectroscopic data with an authentic sample. This makes it likely that a fluoride hydride exchange is taking place leading to a situation in $(C_2F_5)_3SiH$ where a polarity-reversed Si–H bond, i.e. a protic hydrogen atom is generated, that may be exchanged either with the above iminium ion or the protected derivative $[Me_2NCH_2NMe_3]^+$.

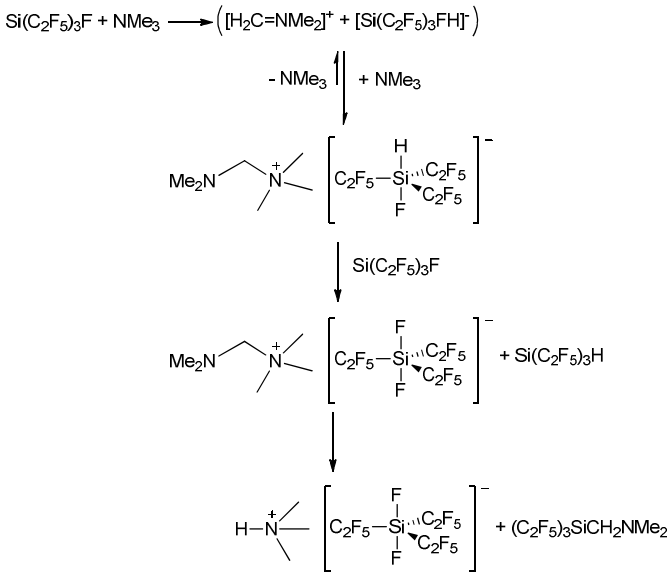

Scheme 2: Proposed sequence for the formation of $(C_2F_5)_3SiCH_2NMe_2$ (**1**) from $(C_2F_5)_3SiF$ and NMe_3.

Model compounds with CH_2-spacer

All compounds with CH_2 as spacer group are colourless liquids. Their solid state structures (Figures 1–3) were obtained by X-ray diffraction of crystals generated by *in situ* crystallisation. Some structural parameters of compounds **1**–**3** are listed in Table 1. The relevant spectroscopic data are provided in the Experimental Section.

The structure of compound **1** shows a silicon atom in a distorted tetrahedral coordination environment (Figure 1). The distortion manifests itself in a twisting of the pentafluoroethyl group (C3–C4) away from the other pentafluoroethyl groups. This is probably due to steric reasons, as this behaviour is also found in the solid state structure of $(C_2F_5)_4Si$.[24]

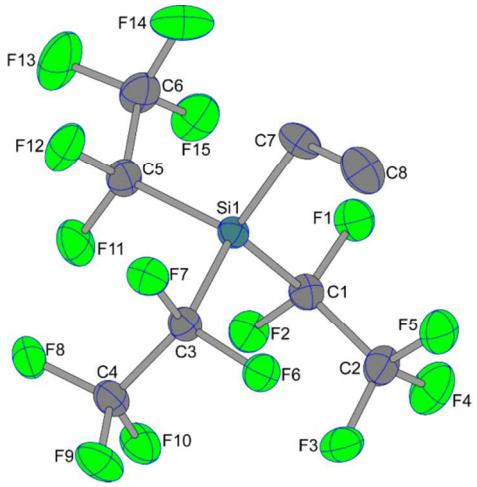

Figure 1: Molecular structure of $(C_2F_5)_3SiCH_2CH_3$ (**1**) in the solid state.

Within the non-fluorinated ethyl group, the Si–C7–C8 angle of 118.6(2)° is substantially larger than an ideal tetrahedral angle (109.5). It reflects the steric congestion at the silicon atom.

Table 1: Bond lengths [Å] and angles [°] for $(C_2F_5)_3SiCH_2CH_3$ as determined by X-ray diffraction (XRD) of compounds **1**, **2** and **3**.

Parameter	**1**	**2**	**3**
Si1–C1	1.938(2)	1.940(2)	1.933(3)
Si1–C3	1.936(3)	1.939(2)	1.941(3)
Si1–C5	1.939(3)	1.938(2)	1.942(3)
Si1–A	1.841(2)	1.861(1)	1.869(3)
Si1–X	2.900(1)	2.619(1)	2.822(3)
A–X	1.527(4)	1.414(2)	1.458(4)
Si1–A–X	118.6(2)	105.4(1)	115.5(2)
C3–Si–A–X	156.1(2)	–56.9(1)	142.6(2)

The structure of compound **2** also shows a silicon atom in a tetrahedral coordination environment (Figure 2). The Si···O distance has a value of 2.619(1) Å The Si–C–O angle with 105.4(1)° is smaller than the tetrahedral angle and slightly smaller than in F_3SiCH_2OMe (Si–C–O 107.1(1)°, and distance Si–O 2.634(2) Å).[14] This points to a stronger interaction between the oxygen and silicon atoms in **2**, despite the highly increased steric demand of C_2F_5 substituents. However, the Si–C–O angle is 13.2° smaller than the Si–C7–C8 angle in reference compound **1**, again indicating some attractive interaction between the silicon and oxygen atoms.

In C_6D_6 solution, the NMR signal of the ^{29}Si nucleus is shifted about 10 ppm to higher field compared to that of compound **1**. This can be explained by the through bond effect of the electronegative methoxy group, but this chemical shift value of –22.4 ppm is still far away from the range of typical pentacoordinate silicon compounds.

The structure of compound **3** shows again a tetrahedral coordination environment about the silicon atom (Figure 3). Its Si–C–N angle adopts a value of 115.3(2)°, which again is still smaller than the corresponding angle of reference compound **1**.

The idealised lone pair of the methyl group deviates from the Si–C–N-plane by 34.4°, making an orbital interaction between Si and N atoms implausible. The bridging CH_2 unit itself is twisted from the N–Si–C5 plane by 11.7°, pointing towards strong steric repulsion of the Me_2N unit with the C_2F_5-substituents.

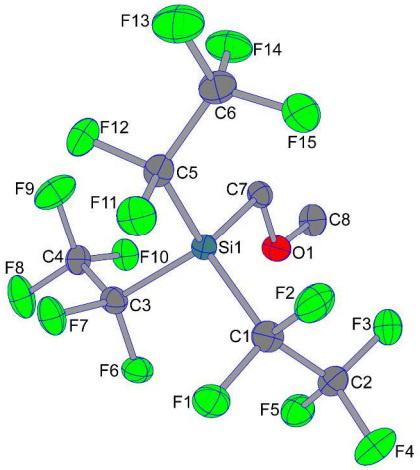

Figure 2: Molecular structure of $(C_2F_5)_3SiCH_2OMe$ (**2**) in the solid state.

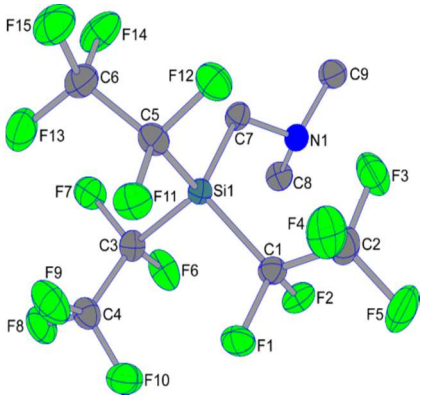

Figure 3: Molecular structure of $(C_2F_5)_3SiCH_2NMe_2$ (**3**) in the solid state.

In C_6D_6 solution the ^{29}Si NMR chemical shift of **3** at –21.8 ppm is very close to the shift of compound **2**, indicating a related chemical environment in solution.

The sum of the C1–Si–C3, C1–Si–C5 and C3–Si–C5 angles, involving all C_2F_5 groups, gives another indication of the interaction between donor and Si atoms. For compound **1** and **3**, this sum has a value of 323°, while in compound **2** this value is compressed to 316° indicating a stronger Si–donor interaction since the sterically bulky substituents have to move closer together.

A model compound with Si–O–N motif

In earlier investigations on ring formation in Si–A–X systems, the aminoxysilanes were those with the most pronounced β-Si···N interactions. In order to show, whether the steric bulk of three pentafluoroethyl substituents would still allow a β-donor site to coordinate and form a neutral pentacoordinate species, we determined the solid state structure of $(C_2F_5)_3SiONMe_2$ (**4**). The asymmetric unit contains two molecules, one of them is shown in Figure 4 (parameters see Table 2).

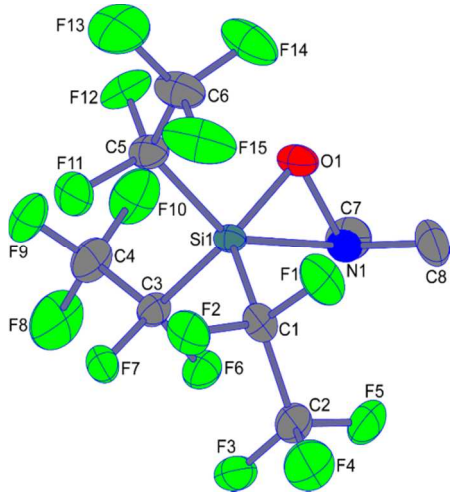

Figure 4: Molecular structure of $(C_2F_5)_3SiONMe_2$ (**4**) in the solid state.

In contrast to the compounds with a CH_2 spacer, the silicon atom in compound **4** clearly shows pentacoordination at the silicon atom. Its Si–O–N angle adopts a remarkably small value of 82.0(1)° and 83.7(1)°, despite the high steric demand of the pentafluoroethyl substituents. This indicates strong interactions between the silicon and nitrogen atoms.

Also, probably due to the more ionic character of the Si–O bond and according to the rule of Bent, the Si–C bonds are all elongated by about 0.01–0.02 Å compared to compounds **1**–**3**. Again, the sum of the C–Si–C angles shows a clearly decreased value of 311° resp. 316°, the smallest in the set of these compounds, showing the closest proximity of the pentafluoroethyl substituents.

Table 2: Bond lengths [Å] and angles [°] for $(C_2F_5)_3SiONMe_2$ as determined by X-ray diffraction (XRD) of compound **4**.

Parameter	4
Si1–C1	1.951(2)
Si1–C3	1.955(2)
Si1–C5	1.945(2)
Si1–A	1.634(2)
Si1–X	2.060(1)
A–X	1.503(2)
Si1–A–X	82.0(1)
C3–Si–A–X	179.1(1)

In C_6D_6 solution the ^{29}Si NMR signal (–67 ppm) is shifted to much higher field than that in **1**, **2** or **3**. Compared to $(C_2F_5)_3SiOEt$ with a chemical shift of –48 ppm and $(C_2F_5)_2Si(OEt)_2$ with a chemical shift of –66 ppm (both in MeCN-D_3), this shift seems to be mainly due to the exchange of a C by an O binding atom and not so much due to pentacoordination.[24] Pentacoordinated silicates typically exhibit chemical shift values at higher field than –90 ppm.

Theoretical investigations and experimental gas-phase structure of 4

Structure prediction by quantum-chemistry

Previous studies in our group aimed at finding reasons for the increased reactivity in the so-called *α*-silanes on the basis of the electronic situation between the silicon and donor atoms. Different quantum-chemical methods have been used so far. The interaction between the two relevant atoms has been described by means of NBO analyses, interpretation of the topology of calculated electron density distributions along the AIM theory and also other groups using the so-called *σ*-hole concept, i.e. by interpretation of the electrostatic potentials at the interacting partners.[25]

Still, no theoretical model found conclusive explanation for all compounds under investigation. For instance, the electron density distributions in the model compounds $F_3SiONMe_2$ and $(CF_3)F_2SiONMe_2$ did not show bond critical points (bcp), although there are clear attractive interactions between Si and N atoms.[9,10] Further calculations indicated a deviation of the location of the donor's lone pair from a possible bond axis. DFT calculations indicated, that the decreased angles could be due to electrostatically or dipolar induced effects.[14,26]

Table 3: Comparison of experimental XRD with theoretical values (bond lengths are in Å, angles are in degrees) of some most important parameters of compounds **1**–**4**.

	Parameter	XRD	B3LYP	PBE0	MP2
1	Si–C–C	118.6(2)	116.5	117.4	116.5
	Si–C	1.841(2)	1.876	1.867	1.862
	C–C	1.527(4)	1.540	1.529	1.534
	Si···C	2.900(1)	2.910	2.907	2.893
2	Si–C–O	105.4(1)	106.1	107.1	104.3
	Si–C	1.861(1)	1.891	1.883	1.877
	C–O	1.414(2)	1.414	1.401	1.413
	Si···O	2.619(1)	2.657	2.657	2.613
3	Si–C–N	115.5(2)	112.4	116.4	111.8
	Si–C	1.869(3)	1.893	1.892	1.878
	C–N	1.458(4)	1.468	1.446	1.463
	Si···N	2.822(3)	2.803	2.847	2.777
4	Si–O–N	82.0(1)/ 83.7(1)	105.0	102.6	83.6
	Si–O	1.634(1)/1.635(1)	1.655	1.644	1.666
	O–N	1.503(2)/1.500(2)	1.486	1.459	1.490
	Si···N	2.060(1)/2.093(1)	2.494	2.425	2.107

Yet, for compounds with a CH_2 spacer, no significant interactions between silicon and donor atoms were found in their ground state structures. The bond angles were not found to be smaller although this would have been expected. However, they were never referenced against a structurally similar benchmark compound without a donor atom, yet they showed a flat bending potential for decreasing the Si–A–X angle.[15,17]

To explain the found structural motifs, we carried out quantum-chemical investigations to find out whether the discussed increased Si–C–C and Si–C–N angles in compounds **1** and **3** are simply due to the high steric demand of the pentafluoroethyl groups or if electronic factors are playing a role as well.

First of all, the molecular structures of the title compounds have been optimised on the B3LYP/6-31G(d,p) level of theory starting from the experimental XRD geometries. The reason for using the DFT[27] approximation was that in our further work corresponding wave functions are easy to analyse in terms of NBO[16] and IQA[28] models in contrast to those from correlated methods like MP2.[29] Following the geometry optimizations, harmonic frequencies calculations were performed to prove that the found structures are at equilibrium. The results (Table 3) are generally comparable to those from XRD studies with the exception of the most extreme Si–O–N angle in **4**, for which the used approximations – in particular DFT – predict much larger values. In principle, it is difficult to compare experimental solid state structures and those calculated for isolated molecules. This is particularly true for compounds involving interactions that depend on the polarity of their surrounding, like compounds with dative bonds or weak donor-acceptor-type interactions.[30] Nevertheless, for testing purposes we have performed more calculations using a DFT functional, PBE0[31] and an increased basis set, namely PBE0/cc-pVTZ. This improved the agreement slightly, as can be seen in Table 3. Finally, the most expensive MP2/cc-pVTZ calculations were performed. Only on this level of theory was it possible to get close to the experimental solid-state value of the Si–O–N angle. However, as mentioned above, the true gas-phase value must be larger than the solid-state values. For this reason we have undertaken the attempt to determine the structure of **4** in the state of free molecules experimentally by gas electron diffraction.

Structure of 4 by gas electron diffraction

Preliminary calculations on the B3LYP/6-31G(d,p) level of theory revealed five conformations of $(C_2F_5)_3SiONMe_2$ (**4**) differing in their torsional angles φ(C–C–Si–O) related to the three C_2F_5 groups (see Table S1, ESI). The first conformer is predicted to be the most abundant (Table S2) and corresponds to that found in the crystal phase. Consequently, five different models (conf1 – conf5) have been tested in the analyses of the experimental electron scattering intensities. They all gave relatively small and similar *R* factors indicating the inability to determine experimentally the most stable conformation on the basis of GED data. Additionally, the analysis of the radial distribution curves showed that the molecules are highly flexible in the gas phase since the experimental radial distribution curve has no distinct peaks in region between 3.8 and 8.0 Å (Figure 5). This is mainly due to the large number of non-bonded F···F distances in addition to conformational richness and flexibility. As a result, the refined vibrational amplitudes for atomic pairs with corresponding interatomic distances were about four times larger than their quantum-chemically predicted values. At this point model conf5 was formally the best fitting one with the lowest *R* factor. Consequently, a dynamic model was set up on its basis. For this purpose a potential function along the torsional angle φ(O2–Si1–C12–C15) was calculated in B3LYP/6-31G(d,p) approximation (Figure S2). A total of 18 pseudo-conformers, weighted according to Boltzmann's law, were generated. Refinement of this model proceeded in the same way as for the previously described static models with the exception of a fixed torsion angle φ(O2–Si1–C12–C15) for all pseudo-conformers. The obtained *R* factor was, however, higher than in the corresponding static model and the difference radial distribution curve did not improve (see Figure 5). An attempt to refine the potential function did not improve the agreement either. A significantly better model would require at least a potential hypersurface for all three torsion angles φ(O2–Si1–C–C). Constructing such a model was, however, impossible due to the very high computational costs.

Finally, it was decided to construct a static model conf1MD, which was a modified model conf1 with interatomic vibrational amplitudes and corrections obtained from molecular dynamics (MD) simulations. The standard procedure for calculation of these quantities implemented in the Shrink program[32] uses the first-order perturbation theory,[33] which assumes that all vibrations in a molecule have small amplitudes. This is obviously not the case for the species under investigation. Calculation of amplitudes and corrections from MD trajectories has no such requirement and can produce quantities that effectively account for the floppiness of the molecule.[34] The ab initio MD simulation for $(C_2F_5)_3SiONMe_2$ was performed using the B3LYP/6-31G(d,p) approximation with time steps d*t* = 1 fs. In total a

10.86 ps long trajectory has been collected and used for the calculation of vibrational amplitudes and corrections (see Table S4). Refinement of the conf1MD model (Figure 6) gave the best agreement with the experimental data (Figure 5). The obtained geometrical parameters are listed in Table 1. This structure can, however, be considered only as an effective one due to the very high flexibility of the molecules and the inability to model this appropriately. All refined bond lengths in the molecule and angles in C_2F_5 groups can be considered as semi-experimental equilibrium parameters. The rest of the refined parameters have effective values although vibrational corrections to equilibrium structure have been used. Very large standard deviations for the refined torsion angles can be explained by (a) deficiency of the model due to high amplitude motions in the molecule and (b) by the absence of peaks on the radial distribution curve in the conformationally sensitive region above ca. 4 Å.

Although this seemingly indicates a failure of determining the gas-phase structure of **4**, it is an experimental proof of its complexity and floppiness.

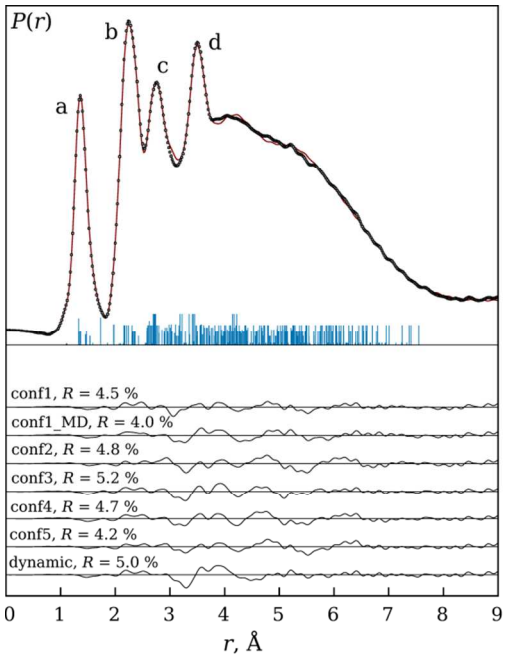

Figure 5: Radial distribution function of $(C_2F_5)_3SiONMe_2$ (**4**). Dots correspond to experimental data, line is the model. Vertical bars show all interatomic distances in the molecule. Most important contributions were (a) bonded C–H, C–F, C–N, N–O, C–C and Si–O atoms, (b) geminal F···F in CF_3 groups, C···O and C···F atoms, (c) geminal Si···F and vicinal F···F atoms in C_2F_5 groups in gauche orientation, (d) Si···F (F in CF_3 groups), vicinal F···F atoms in C_2F_5 groups in *anti*-orientation. Difference curves and corresponding R factors for all tested models are in the bottom.

QUANTUM-CHEMICAL DESCRIPTION OF BONDING IN 1–4

Wave functions obtained for equilibrium structures on the B3LYP/6-31G(d,p) level were further used in IQA and NBO analyses. This was dictated mostly by the fact, that in the IQA method as implemented in AIMAll program[36] the correct calculation of exchange-correlation energy is programmed only for the LSDA[37] and B3LYP[38] functionals. Wave functions from correlated methods cannot be fully correctly used in the IQA and are also less useful in the NBO model.

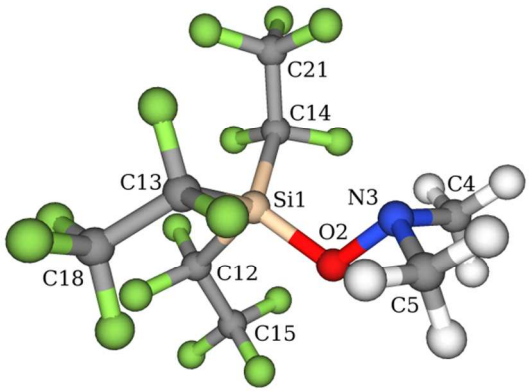

Figure 6: Effective gas-phase structure of $(C_2F_5)_3SiONMe_2$ (**4**) refined in the conf1MD model.

As expected, NBO calculations for reference compound **1** show no significant interactions between orbitals localised on the Si–CH_2–CH_3 fragment. The most significant interactions are between orbitals corresponding to lone pairs of electrons on the fluorine atoms and adjacent anti-bonding σ^*(C–F) orbitals. The respective stabilization energies $E^{(2)}$ estimated from the second order perturbation theory analysis are in the range 10.9 – 18.1 kcal mol^{-1}. This is a common feature for all the compounds discussed here.

The situation in compound **2** could be potentially more interesting due to the lone pairs of electrons on the oxygen atom. In our calculations, however, no strong interactions were found between the silicon and oxygen atoms. The most dominant one was between one of the oxygen lone pairs and a Rydberg orbital (1-center anti-bonding orbital localised on an atom) of the carbon atom in the Si–C–O unit with $E^{(2)}$ = 2.6 kcal mol^{-1}.

In compound **3** the electron lone pair on the nitrogen atom interacts mostly with anti-bonding orbitals localised on those C–H bonds of CH_2 and CH_3 groups which are approximately perpendicular to the plane formed by three carbon atoms of the –$CH_2N(CH_3)_2$ moiety. The corresponding $E^{(2)}$ energy is 7.7 kcal mol^{-1} on average.

Calculations for compound **4** show the expected n(F)→σ^*(C–F) and n(N)→σ^*(C–H) interactions as in compound **3**. In addition, there were also weak n(N)→σ^*(Si–O) with $E^{(2)}$ = 3.0 kcal mol^{-1} and n(N)→σ^*(Si–C5) interaction with $E^{(2)}$ = 3.8 kcal mol^{-1}. The latter is shown in Figure 5. This pair of orbitals is the only one in the NBO model which can be related to the experimentally observed attractive interaction between silicon and nitrogen atoms in **4**.

Electron densities of all compounds calculated on the B3LYP/6-31G(d,p) level were analysed in terms of AIM theory. In none of them bond critical points (bcps) were found for Si···X atomic pairs, indicating the absence of corresponding bonding. The latter statement is also supported by electron

delocalization indices calculated in the AIM model (bond indices in case of bonded atoms). For the Si···X pairs they were in the range between 0.15 and 0.24. The lowest value belongs to the pair Si···C in **1**, while the largest value is for Si···N in **4**. Among all bcps found in **1**–**4** there were also such for F···F and F···H contacts. The values of their electron densities (around 0.008 a.u. on average) and small positive Laplacians in these bcps indicate very weak closed-shell type interactions.

In the absence of bcps for the Si···X pairs in **1**–**4** the Reduced Density Gradient (RDG) analysis[38] is useful. The RDG ($s = 1/(2(3\pi^2)^{1/3})|\nabla\rho|/\rho^{4/3}$) together with its derivative is one of essential quantities in DFT theory.[39] The RDG shows deviations of electron density from the homogeneous electron distribution and can be used for identifying non-covalent interactions.[35,37] Regions of low RDG values are associated with either attractive or repulsive interactions depending on the sign of the second eigenvalue λ_2 of the electron-density Hessian (matrix of second derivatives). Negative and positive λ_2 correspond to attractive and repulsive interactions, respectively. In bcps the RDG is zero by definition. There can be, however, regions between atoms where the RDG is close to zero and λ_2 is negative. Such areas are called "uncompleted links" or "quasi-bonding channels".[40] The RDG analysis has been applied to compounds **1**–**4**. Figures 6 and 7 show the calculated RDG and electron density with mapped sign[λ_2] values in compound **4**.

As can be seen, the regions of bcps corresponding to the Si–O and O–N bonds have low RDGs (zero in bcps) and negative λ_2 values. This characterises attractive bonding pattern. In the area between the silicon and nitrogen atoms the RDG is relatively large (0.4–0.7 arb. units) and λ_2 is partially positive. These two factors allow concluding that the electron density between the silicon and nitrogen atoms is far from the condition, when it is possible to form a bond. Analogous analyses have been performed for compounds **1**–**3** with similar results (see SI for Figures).

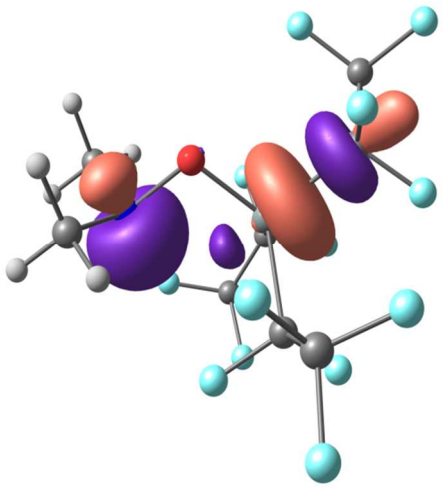

Figure 5: The electron lone pair orbital on the nitrogen atom and the anti-bonding σ*(Si-C) orbital in **4** as calculated by NBO.

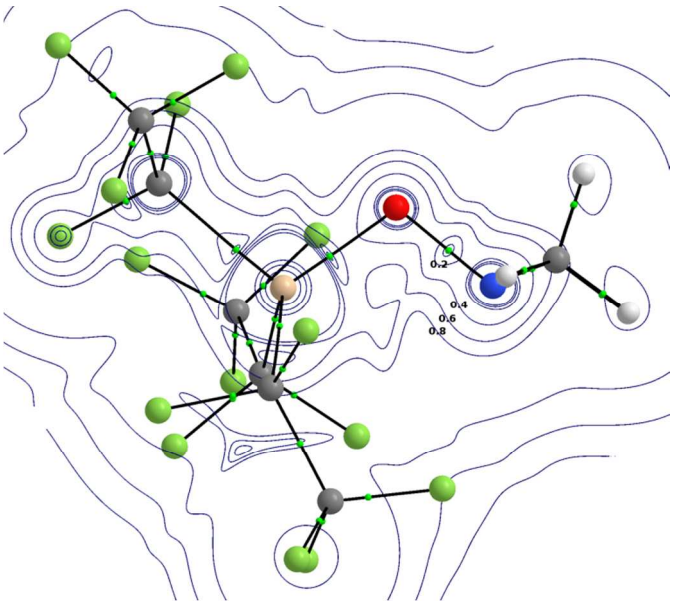

Figure 6: Contour plot of dimensionless RDG of compound **4** in the SiON plane. Values for some iso-lines are shown.

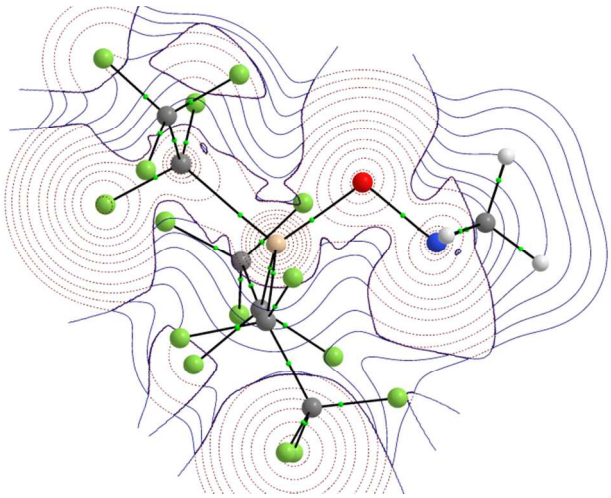

Figure 7: Contour plot of electron density of compound **4** in the SiON plane. The sign of λ_2 (see text) is mapped onto the plot so that the blue solid lines correspond to $\lambda_2 > 0$ and the red dashed lines to $\lambda_2 < 0$, respectively.

Table 4: AIM atomic charges [*e*] for Si–A–X fragments in compounds **1**–**4**.

	δ(Si)	δ(X)	δ(A)
1	2.72	0.09	–0.70
2	2.72	–1.06	–0.16
3	2.71	–0.98	–0.36
4	2.85	–0.57	–1.05

On the other hand, the AIM atomic charges of Si and X atoms (see Table 4) indicate possible mutual attractive electrostatic interactions in compounds **2**–**4**. The Si···C contact in **1** should be repulsive. To analyse this hypothesis in detail IQA calculations were performed. On the basis of the AIM definition of atomic basins in the IQA model the total molecular energy can be unambiguously represented as a sum

of all intra-atomic E(A) and inter-atomic E(A,B) terms: $E_{mol} = \Sigma_A E(A) + \Sigma_{A>B} E(A,B)$. The first type of terms represents energies of atoms in a molecule while the second corresponds to energies of interatomic interactions.

Table 5 compares interatomic interaction terms for the Si–A–X fragments in compounds **1**–**4**. As expected, for bonded Si–A and A–X atom pairs the values are negative, which indicates stabilizing interactions. As regarding the non-bonded Si···X pairs, the positive E(Si,C) term in **1** is destabilizing while in the other compounds the E(Si,X) components are stabilizing. Moreover, the effects of non-bonded Si···X interactions in compounds **2**–**4** are larger than those for the bonded A–X and in some cases comparable to effects of bonded Si–A terms. In the IQA model each interatomic energy term is decomposed to several components $E(A,B) = E_{nn}(A,B) + E_{ne}(A,B) + E_{en}(A,B) + E_{ee}(A,B)$, corresponding to pairwise inter-particle interactions (nucleus A)···(nucleus B), (nucleus A)···(electrons B), (electrons A)···(nucleus B) and (electrons A)···(electrons B), respectively. The latter is further decomposed into the classical Coulomb and quantum exchange-correlation interactions $E_{ee}(A,B) = E^{C}_{ee}(A,B) + E^{xc}_{ee}(A,B)$. The Coulomb part is always positive, while the exchange-correlation term is negative. The latter is also smaller in magnitude than the former but in fact plays an important role in formation of chemical bonds. The absolute value of $E^{xc}_{ee}(A,B)$ is very small for the ionic type of interactions and much larger for polar and non-polar covalent interactions. In application to the title compounds (see Table 5), the absolute values of $E^{xc}_{ee}(Si,X)$ are two orders of magnitude less than those for $E^{xc}_{ee}(Si,A)$ and $E^{xc}_{ee}(A,X)$. Thus, in comparison with bonded Si–A and A–X, the Si···X contacts demonstrate mostly classical electrostatic stabilizing interactions, although without formation of chemical bonds.

Table 5: IQA diatomic interaction energy components and their exchange-correlation contributions [a.u.] for Si–A–X fragments of compounds **1**–**4**.

	E(Si,X)	E(Si,A)	E(A,X)	E^{xc}_{ee}(Si,X)	E^{xc}_{ee} (Si,A)	E^{xc}_{ee} (A,X)
1	0.049	–1.019	–0.302	–0.002	–0.140	–0.301
2	–0.569	–0.639	–0.426	–0.004	–0.135	–0.285
3	–0.503	–0.781	–0.294	–0.004	–0.138	–0.313
4	–0.294	–1.269	–0.182	–0.006	–0.123	–0.309

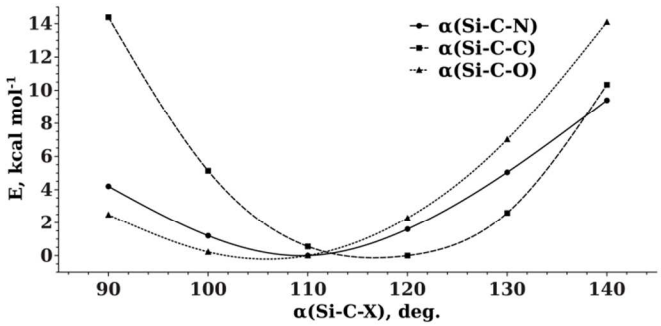

Figure 8: Potential energies for different values of Si–A–X angles in the compounds **1–3**.

To investigate the α-effect in the title compounds further we have calculated potential energy curves for the Si–A–X coordinate at the B3LYP/6-31G(d,p) level. As Figure 8 shows, the potential curves for compounds **2** and **3** are relatively flat in the region of small values of the Si–A–X angles indicating adaptive intramolecular interactions, which compensate large deviations from the equilibrium geometry. This is opposite to the expected steep increase in energy in case of bonded Si···X contacts. The curve for compound **1** is mostly symmetric and, as expected, demonstrates a usual bending potential.

Conclusions

The new model compounds **2** and **3** give further insights into the postulated coordination behaviour of donor atoms which are bonded to a silicon atom via a methylene unit. Taken for themselves, the solid state structures do not indicate an interaction between the silicon and the donor atoms. But in light of the comparison of these structures with reference compound **1** and the results of the quantum chemical calculations, it seems to be plausible to attribute an electrostatic interaction to this class of compounds, after all. Since compound **4** showed a very small Si–O–N angle, purely steric reasons for the behaviour of compounds **1**–**3** can be excluded. Yet, shown by multiple quantum chemical methods, the interactions between the silicon and the donor atoms cannot be characterised by bonds but by electrostatic interactions, thus concluding several previous investigations.

Also, the possible electrostatic impact on the reactivity of this industrially important class of compounds should be further reviewed for more commonly used organosilanes.

Experimental

All experiments were carried out under rigorous inert conditions using Schlenk and Young techniques at vacuum lines. All solvents were dried and distilled before use.

Preparation of $(C_2F_5)_3SiCH_2CH_3$

The compound was prepared according to literature[22] ^{1}H NMR (500 MHz, C_6D_6 25°C): δ 0.91 (m, CH_2), 0.85 (t, CH_3). ^{13}C NMR (126 MHz, C_6D_6 25°C): δ 122.3–114.1 (m, CF_2CF_3) 62.2 (CH_3), 55.0 ($^1J_{SiC}$ = 34 Hz, CH_2). ^{19}F NMR (470 MHz, C_6D_6 25°C): δ –82.2 (CF_3), –121.0 (CF_2). ^{29}Si NMR (99 MHz, C_6D_6 25°C): δ –12.1 (hept, $^2J_{SiF}$ = 33 Hz)

Preparation of $(C_2F_5)_3SiCH_2OMe$

Pentafluoroethane (26.7 mmol) was condensed on a solution of commercially available *n*-butyllithium (16.2 mL, 1.6 mol L^{-1} in *n*-hexane) in diethyl ether (40 mL). This solution was stirred for 2h between –60 and –50°C. After cooling to –72°C, trichloromethoxymethylsilane[11] (1.58 g, 8.4 mmol) was added and stirred for 2.5 h at this temperature. The reaction mixture was allowed to warm to room temperature overnight under stirring. After filtration of the colourless solid lithium chloride, the ether was removed via distillation and the resulting colourless liquid was purified by fractionated distillation to yield 0.816 g (1.9 mmol, 23%) of $(C_2F_5)_3SiCH_2OMe$. ^{1}H NMR (500

MHz, C_6D_6 25°C): δ 3.39 (s, CH_2), 2.88 (s, CH_3). ^{13}C NMR (126 MHz, C_6D_6 25°C): δ 122.3–113.5 (m, CF_2CF_3) 4.2 (CH_2), –1.0 (CH_3). ^{19}F NMR (470 MHz, C_6D_6 25°C): δ –82.6 (CF_3), –120.8 (CF_2). ^{29}Si NMR (99 MHz, C_6D_6 25°C): δ –22.4 (hept, $^2J_{SiF}$ = 34 Hz)

Preparation of $(C_2F_5)_3SiCH_2NMe_2$

Pentafluoroethane (30.3 mmol) was condensed on a solution of commercially available *n*-butyllithium (29.9 mmol) in a mixture of *n*-hexane (18.7ml) and diethyl ether (40 mL). This solution was stirred for 2 h at –55°C. After cooling to –80°C, dimethylaminomethyltrichlorosilane[12] (1.884 g, 9.8 mmol) was added. The reaction mixture was slowly warmed up to room temperature under stirring for 3 d. After filtration from the colourless solid lithium chloride, the remaining brown liquid was purified by fractionated vacuum distillation, yielding 2.337 g (5.3 mmol, 54%) of the clear colourless liquid $(C_2F_5)_3SiCH_2NMe_2$. ^{1}H NMR (500 MHz, C_6D_6 25°C): δ 2.45 (s, CH_2), 1.92 (s, CH_3). ^{13}C NMR (126 MHz, C_6D_6 25°C): δ 122.4–114.0 (m, C_2F_5), 47.9 (CH_3) 41.4 ($^1J_{SiC}$ = 36 Hz, CH_2). ^{19}F NMR (470 MHz, C_6D_6 25°C): δ –81.7 (CF_3), –120.0 (CF_2). ^{29}Si NMR (99 MHz, C_6D_6 25°C): δ –21.8 (hept, $^2J_{SiF}$ = 33 Hz). Anal. calcd. for $C_5H_8F_{15}NSi$: C 23.4, H 1.82, N 3.16; found: C 22.1, H 1.98, N 3.16. IR (gas): ν[cm^{-1}] = 2886 (vw, νCH), 2838 (w, νCH), 2789 (w, νCH), 1470 (vw, δCH$_3$), 1458 (vw, δCH$_3$), 1449 (vw, δCH$_3$), 1404 (vw, δCH$_2$), 1307 (s, νCC), 1231 (vs, νCF$_3$), 1143 (s, νCF$_3$), 1094 (m, ν_sCF$_2$), 1041(m, ν_{as}CF$_2$), 986(m, ν_{as}SiC$_3$), 838 (w, ν_sNC$_3$), 746 (w, δCF$_3$), 615 (w, δCF$_2$), 559 (w), 481 (w).

Alternative synthesis of $(C_2F_5)_3SiCH_2NMe_2$ by reaction of $Si(C_2F_5)_3F$ with NMe_3

In a 100 ml glass ampoule with Young valve NMe_3 (0.30 g, 5.1 mmol) was condensed to $Si(C_2F_5)_3F$ (0.95 g, 2.4 mmol). The reaction mixture was stirred for 12 h. All volatiles were removed from the reaction mixture. Removal of the excess of NMe_3 at 0 °C from the volatiles yielded $Si(C_2F_5)_3CH_2NMe_2$ (0.53g 1.2 mmol, 50% related to $Si(C_2F_5)_3F$) as a colourless liquid. The spectroscopic data were identical to the ones obtained from the first method of synthesis.

Preparation of $(C_2F_5)_3SiONMe_2$

Pentafluoroethane (320 mmol) was condensed onto a frozen solution of commercially available *n*-butyllithium (155 mL, 2 mol L^{-1} in *n*-pentane) in diethyl ether (400 mL) at –196°C and allowed to warm to –60°C. This solution was stirred for 3 h between –60 and –50°C. Trichloro(dimethylaminoxy)silane (19.43 g, 99.89 mmol) was condensed onto the frozen solution and after warming to –40°C the resulting solution was kept at this temperature overnight. It was stirred further for 2 h at –20°C. After filtration of the colourless solid lithium chloride, the ether was removed via distillation and the resulting colourless liquid was purified by fractionated distillation to yield 17.869 g (40.1 mmol, 40.2%) of $(C_2F_5)_3SiONMe_2$. ^{1}H NMR (500 MHz, C_6D_6 25°C): δ 2.24 (s, CH_3). ^{13}C NMR (126 MHz, C_6D_6 25°C): δ 122.6–113.2 (m, C_2F_5), 50.3 (CH_3). ^{19}F NMR (470 MHz, C_6D_6 25°C): δ –81.7 (CF_3), –122.1 (CF_2). ^{29}Si NMR (99 MHz, C_6D_6 25°C): δ –67.3 (hept, $^2J_{SiF}$ = 38 Hz).

Calculations

Quantum-chemical calculations were performed using Gaussian 09[41] and Firefly 8[42] program packages. The NBO calculations were done using the NBO module[43] incorporated in the Firefly program. The IQA and AIM calculations were performed with the AIMAll program suite.[35] For molecular dynamics (MD) simulations US GAMESS 2013 program[44] was used. The required in GED structural analyses mean square amplitudes of interatomic variations and corresponding corrections have been obtained by processing MD trajectories taking into account quantum effects with a new program Qassandra.

Gas electron diffraction

The gas electron diffraction patterns were measured with the improved Balzers Eldigraph KD-G2 gas-phase electron diffractometer[45] at Bielefeld University. Table S3 lists the experimental GED details. Diffraction patterns were recorded on Fuji BAS-IP MP2 2025 imaging plates, which were scanned using a calibrated Fuji BAS-1800II scanner. The intensity curves (Figure S3) were retrieved from the scanned diffraction images by applying a method described earlier.[46] Sector function and electron wavelength were calibrated[47] using CCl_4 diffraction patterns, recorded along with the substance under investigation. Experimental amplitudes were refined in groups (see Table S4). For this purpose scale factors (one per group) were used as independent parameters. The ratios between different amplitudes in one group were fixed at the theoretical values.

Single-crystal X-ray diffraction

Single crystals were crystallized by in-situ methods directly in capillaries on the diffractometer (Agilent Supernova EOS for **1**, **3** and **4**, Nonius Kappa CCD for **2**). This was achieved by first establishing a solid-liquid equilibrium close to the melting point, then melting all solid but a tiny crystal seed (using a thin copper wire as external heat source) followed by slowly cooling until the whole capillary was filled with a single crystalline specimen. Mo-Kα (λ = 0.71073 Å) was used for all measurements. Using Olex2[48] the structures were solved and refined with SHELX-97[49]. Crystal and refinement details, as well as CCDC numbers are provided in Table 6. CCDC 1402070 – 1402073 contains the supplementary crystallographic data for this paper. These data can be obtained free of charge from The Cambridge Crystallographic Data Centre via www.ccdc.ac.uk/data_request/cif.

Table 6 Experimental details for the X-ray diffraction experiments.

Compound number	**1**	**2**	**3**	**4**
Empirical formula	$C_8H_5F_{15}Si$	C_8 H_5 F_{15} O Si	$C_9H_8F_{15}NSi$	$C_8H_6F_{15}NOSi$
Formula weight [g mol^{-1}]	414.21	430.21	443.25	445.23
Temp. of solid-liquid equilibrium [K]	272.0(1)	218.0(1)	155.0(1)	239.8(1)
Temp. of measurement [K]	100.0(1)	100.0(2)	100.0(1)	150.0(1)
Crystal system	orthorhombic	monoclinic	monoclinic	triclinic
Space group	$P2_12_12_1$	$P2_1/n$	$P2_1/n$	$P\bar{1}$
a/[Å]	8.5336(3)	10.2956(4)	7.6077(3)	8.0664(3)
b/[Å]	8.7427(3)	8.9617(2)	15.7881(7)	13.2774(13)
c/[Å]	18.1777(6)	15.4672(6)	12.7448(6)	14.9990(10)
α/[°]				105.422(7)
β/[°]		90.9977(16)	92.425(4)	91.660(5)
γ/[°]				104.381(6)
Volume [Å^3]	1356.18(8)	1426.88(8)	1529.41(12)	1492.26(19)
Z	4	4	4	4
ρ_{calc} [g cm^{-3}]	2.029	2.003	1.925	1.982
μ [mm^{-1}]	0.347	0.339	0.317	0.330
F(000)	808.0	840	872.0	872.0
Crystal size [mm^3]	0.30 × 0.30× 0.30	0.30 x 0.30 x 0.30	0.30 × 0.20 × 0.18	0.3 × 0.22 × 0.20
2Θ range [°]	4.5 to 55.3	3.0 to 27.46 deg	5.0 to 58.0°	3.7 to 60.1°
Reflections collected	48786	13230	16214	87610
Independent reflections	3118	3163	2685	8724
R_{int}	0.0681	0.034	0.0430	0.0276
Reflections with $I \geq 2\sigma$ (I)	3039	2402	2142	7516
Data/restraints/parameters	3118/0/218	3163 / 0 / 227	2685/0/267	8724/0/581
Goodness-of-fit on F^2	1.168	0.971	1.095	1.039
Final R_1 [$I \geq 2\sigma$ (I)]	0.0374	0.0301	0.0407	0.0394
Final wR_2 [$I \geq 2\sigma$ (I)]	0.1015	0.0710	0.0944	0.0925
Final R [all data]	0.0385	0.0459	0.0567	0.0460
Final wR_2 [all data]	0.1025	0.0749	0.1040	0.0967
ρ_{fin} max/min [e Å^{-3}]	0.56/-0.24	0.280/-0.304	0.40/-0.29	0.44/-0.51
remarks	Flack parameter –.04(17)			diorder of one C_2F_5 group
CCDC	1402070	1402071	1402072	1402073

Acknowledgements

This work was supported by Deutsche Forschungsgemeinschaft (core facility GED@BI). Authors thank HPC facilities at the Universität zu Köln for providing computational time and programs. We are grateful to Solvay GmbH (Hannover, Germany) for providing pentafluoroethane.

Notes and references

Inorganic and Structural Chemistry, Centre for Molecular Materials CM_2, Fakultät für Chemie, Universität Bielefeld, Universitätsstraße 25, 33615 Bielefeld (Germany); E-mail: mitzel@uni-bielefeld.de.

Electronic Supplementary Information (ESI) available: Tables of calculated torsional angles, relative energies and abundancies for the conformers of $(C_2F_5)_3SiONMe_2$ and graphs of its potential functions as well as total and molecular electron scattering intensity functions. See DOI: 10.1039/b000000x/

1 N. Egorochkin, S. E. Skobeleva, E. I. Sevast'yanova, I. G. Kosolapova, V. D. Sheludyakov, E. S. Rodionov and A. D. Kirilin, *Zh. Obshch. Khim*. 1976, **46**, 1795.

2 G. Mital and R. R. Gupta, *J. Am. Chem. Soc*. 1969, **91**, 4664.

3 J. M. Bellama and A. G. MacDiarmid, *J. Organomet. Chem.*1970, **24**, 91.

4 a) E. W. Randall, C. H. Yoder and J. J. Zuckerman, *lnorg. Chem.* 1967, **6**, 744; b) Z. Pacl, M. Jakoubkova, Z. Papouskova and V. Chvalovsky, *Collect. Czech. Chem. Commun.* 1971, **36**, 1588; c) A. Marchand, J. Mendelsohn, M. Lebedeff and J. Valade, *J. Organomet. Chem.* 1969, **17**, 379.

5 a) R. G. Kostyanovskii and A. K. Prokov'ev, *Dokl. Akad. Nauk SSSR*, 1965, **164**, 1054 – 1057; b) V. V. Kharpov, V. I. Gol'danskii, A. K. Prokov'ev and R. G. Kostyanovskii *Zh. Obshch. Khim.* 1967, **37**, 3.

6 a) G. Wilkinson and F. G. A. Stone, E. W. Abel *Comprehenshive Organometallic Chemistry*, 1st Ed. Pergamon Press: Oxford, 1982, Vol. 2, p. 412; b) M. G. Voronkov, T. V. Kashik, E. Y. Lukevits, E. S. Deriglazova, A. E. Pestunovich and R. Y. Moskovich, *Zh. Obshch. Khim.* 1974, **44**, 778; c) S. Y. Khorshev, A. N. Egorochkin, E. I. Sevast'yanova, N. S. Ostasheva and O. V. Kuz'min, O. V. *Zh. Obshch. Khim.* 1976, **46**, 1795; d) V. P. Feshin and M. G. Voronkov, *J. Mol. Struct.* 1982, **83**, 317.

7 a) A. Bauer, T. Kammel, B. Pachaly, O. Schäfer, W. Schindler, V. Stanjek and J. Weis, *Organosilicon Chemistry V*, Wiley-VCH, Weinheim, 2003, p. 527; b) *One step ahead – organofunctional silanes from Wacker*, Brochure of the Wacker company: www.wacker.com/internet/webcache/de_DE/BrochureOrder/GENIOSIL_Brosch_e.pdf; c) W. Schindler, *Adhaes.–Kleben Dichten*, 2004, **48**, 29.

8 A. Berkefeld, C. Fonseca Guerra, R. Bertermann, D. Troegel, J. O. Daiß, J. O. Stohrer, F. M. Bickelhaupt and R. Tacke, *Organometallics* 2014, **33**, 2721–2737.

9 N. W. Mitzel, U. Losehand, A. Wu, D. Cremer and D. W. H. Rankin, *J. Am. Chem. Soc.* 2000, **122**, 4471–4482.

10 N. W. Mitzel, K. Vojinović, R. Fröhlich, T. Foerster, H. E. Robertson, K. B. Borisenko and D. W. H. Rankin, *J. Am. Chem. Soc.* **2005**, 127, 13705–13713.

11 R. F. W. Bader, *Atoms in Molecules: A Quantum Theory*, Clarendon Press, Oxford, 1990.

12 D. Winkelhaus, Yu. V. Vishnevskiy, R. J. F. Berger, H.-G. Stammler, B. Neumann and N. W. Mitzel, *Z. Anorg. Allg. Chem.* 2013, **639**, 2086–2095.

13 K. Vojinovic, L. McLachlan, D. W. H. Rankin and N. W. Mitzel, *Chem. Eur. J.* 2004, **10**, 3033–3042.

14 N. W. Mitzel, *Z. Naturforsch.* **2003**, 58b, 759–763.

15 N. W. Mitzel, K. Vojinović, T. Foerster, H. E. Robertson, K. B. Borisenko and D. W. H. Rankin, *Chem. Eur. J.* **2005**, 11, 5114–5125.

16 J. P. Foster and F. Weinhold, *J. Am. Chem. Soc.* 1980, **102**, 7211–7218.

17 M. Woski, R. J. F. Berger and N. W. Mitzel, *Dalton Trans.* 2008, **41**, 5652–5658.

18 S. A. Hayes, R. J. F. Berger, B. Neumann, N. W. Mitzel, J. Bader and B. Hoge, *Dalton Trans.* 2010, **39**, 5630–5636.

19 K. G. Sharp and T. D. Coyle, *Inorg. Chem.* **1972**, 11, 1259–1264.

20 a) M. Heinrich, A. Marhold, A. Kolomeitsev, A. Kadyrov, G.-V. Röschenthaler and J. Barten (Bayer AG), *DE 10128703A 1*, 2001; b) M. H. Königsmann, *Dissertation*, Universität Bremen, 2005; c) A. A. Kolomeitsev, A. A. Kadyrov, J. Szczepkowska-Sztolcman, H. Milewska, G. Bissky, J. A. Barten and G.-V. Röschenthaler, *Tetrahedron Lett.* 2003, **44**, 8273–8277.

21 B. Waerder, S. Steinhauer, B. Neumann, H.-G. Stammler, A. Mix, Y. V. Vishnevskiy, B. Hoge and N. W. Mitzel, *Angew. Chem.* **2014**, *129*, 11824-11828; *Angew. Chem. Int. Ed.* **2014**, *53, 11640-11644*.

22 S. Steinhauer, H.-G. Stammler, B. Neumann, N. Ignat'ev and B. Hoge, *Angew. Chem.* **2014**, 126, 573–575.

23 S. Steinhauer, T. Böttcher, N. Schwarze, B. Neumann, H.-G. Stammler and B. Hoge, *Angew. Chem.* 2014, 126, 13485-13488.

24 S. Steinhauer, B. Hoge, *unpublished results*.

25 J. S. Murray, M. C. Concha and P. Politzer, *J. Mol. Model.* 2011, **17**, 2151–2157.

26 N. W. Mitzel, C. Kiener and D. W. H. Rankin, *Organometallics* 1999, **18**, 3437–3444.

27 R. G. Parr and W. Yang, *Density-Functional Theory of Atoms and Molecules*, Oxford University Press, USA, 1989.

28 M. A. Blanco, A. Martín Pendás and E. Francisco, *J. Chem. Theory Comput.* 2005, **1**, 1096–1109.

29 C. Møller and M. S. Plesset, *Phys. Rev.* 1934, **46**, 618–622.

30 a) K. R. Leopold, M. Canagaratna and J. A. Phillips, *Acc. Chem. Res.* 1997, **30**, 57; b) H. Jiao and P. v. R. Schleyer, *J. Am. Chem. Soc.* 1994, **116**, 7429.

31 J. P. Perdew, K. Burke and M. Ernzerhof, *Phys. Rev. Lett.* 1996, **77**, 3865-3868.

32 V. A. Sipachev, *Struct. Chem.* 2000, **11**, 167–172.

33 a) V. A. Sipachev, *J. Mol. Struct.* 2001, **567–568**, 67–72; b) V. A. Sipachev, *J. Mol. Struct.* 2004, **693**, 235–240.

34 a) D. A. Wann, R. J. Less, F. Rataboul, P. D. McCaffrey, A. M. Reilly, H. E. Robertson, P. D. Lickiss and D. W. H. Rankin, *Organometallics*, 2008, **27**, 4183; b) D. A. Wann, A. V. Zakharov, A. M. Reilly, P. D. McCaffrey and D. W. H. Rankin, *J. Phys. Chem. A*, 2009, **113**, 9511; c) A. V. Zakharov, Y. V. Vishnevskiy, N. Allefeld, J. Bader, B. Kurscheid, S. Steinhauer, B. Hoge, B. Neumann, H.-G. Stammler, R. J. F. Berger and N. W. Mitzel, *Eur. J. Inorg. Chem.*, 2013, **19**, 3392.

35 T. A. Keith, AIMAll (Version 14.06.21) TK Gristmill Software, Overland Park KS, USA, 2014.

36 S. H. Vosko, L. Wilk and M. Nusair, *Can. J. Phys.* 1980, **58**, 1200–1211.

37 A. D. Becke, *J. Chem. Phys*. 1993, **98**, 5648–5652.

38 E. R. Johnson, S. Keinan, P. Mori-Sánchez, J. Contreras-García, A. J. Cohen and W. Yang, *J. Am. Chem. Soc.* 2010, **132**, 6498–6506.

39 P. Hohenberg and W. Kohn, *Phys. Rev.* 1964, **136**, 864–871.

40 E. V. Bartashevich, A. Martín Pendás and V. G. Tsirelson, *Phys. Chem. Chem. Phys*. 2014, **16**, 16780–16789.

41 M. J. Frisch, G. W. Trucks, H. B. Schlegel, G. E. Scuseria, M. A. Robb, J. R. Cheeseman, G. Scalmani, V. Barone, B. Mennucci, G. A. Petersson, H. Nakatsuji, M. Caricato, X. Li, H. P. Hratchian, A. F. Izmaylov, J. Bloino, G. Zheng, J. L. Sonnenberg, M. Hada, M. Ehara, K. Toyota, R. Fukuda, J. Hasegawa, M. Ishida, T. Nakajima, Y. Honda, O. Kitao, H. Nakai, T. Vreven, J. A. Montgomery, Jr., J. E. Peralta, F. Ogliaro, M. Bearpark, J. J. Heyd, E. Brothers, K. N. Kudin, V. N. Staroverov, T. Keith, R. Kobayashi, J. Normand, K. Raghavachari, A. Rendell, J. C. Burant, S. S. Iyengar, J. Tomasi, M. Cossi, N. Rega, J. M. Millam, M. Klene, J. E. Knox, J. B. Cross, V. Bakken, C. Adamo, J. Jaramillo, R. Gomperts, R. E. Stratmann, O. Yazyev, A. J. Austin, R. Cammi, C. Pomelli, J. W. Ochterski, R. L. Martin, K. Morokuma, V. G. Zakrzewski, G. A. Voth, P. Salvador, J. J. Dannenberg, S. Dapprich, A. D. Daniels, O. Farkas, J. B. Foresman, J. V. Ortiz, J. Cioslowski and D. J. Fox, Gaussian 09, Revision D.01, Gaussian, Inc., Wallingford CT, 2013.

42 A. A. Granovsky, Firefly version 8, www http://classic.chem.msu.su/gran/firefly/index.html

43 E. D. Glendening, J. K. Badenhoop, A. E. Reed, J. E. Carpenter, J. A. Bohmann, C. M. Morales and F. Weinhold, NBO 5.G., Theoretical Chemistry Institute, University of Wisconsin, Madison, WI, 2004; http://www.chem.wisc.edu/~nbo5

44 M. W. Schmidt, K. K. Baldridge, J. A. Boatz, S. T. Elbert, M. S. Gordon, J. H. Jensen, S. Koseki, N. Matsunaga, K. A. Nguyen, S. Su, T. L. Windus, M. Dupuis, J. A. Montgomery, *J. Comput. Chem.* **1993**, *14*, 1347-1363.
45 R. J. F. Berger, M. Hoffmann, S. A. Hayes, N. W. Mitzel, *Z. Naturforsch*. 2009, **64b**, 1259–1268.
46 Yu. V. Vishnevskiy, *J. Mol. Struct.* 2007, **833**, 30–41.
47 Yu. V. Vishnevskiy, *J. Mol. Struct.* 2007, **871**, 24–32.
48 O. V. Dolomanov, L. J. Bourhis, R. J. Gildea, J. A. K. Howard and H. Puschmann, *J. Appl. Crystallogr*. 2009, **42**, 339–341.
49 G. M. Sheldrick, *Acta Crystallogr.* 2008, **A64**, 112–122.

